UNIVERSITÁ DEGLI STUDI DI ROMA
TOR VERGATA

Macroarea di Ingegneria

Mechanical Engineering Master's Thesis

Analysis of Vortex Induced Vibration of a thermowell by high fidelity FSI numerical analysis based on RBF structural modes embedding

Advisor:

Prof. Marco Evangelos Biancolini

Co-Advisor:

Ph.D. Ubaldo Cella

Candidate:

Alessandro Felici

Academic year 2019/2020

Università di Roma Tor Vergata

Contents

Introduction

- Today the need for developing multi-physics approaches in order to address modern and complex design challenges is rising. A typical multi-physics phenomenon is the interaction between a fluid and a structure, that occurs according to the following options: it can be the working principle of the considered component, it can be due to the lightweight design of the structure or else it can be exploited to finely tune the design.
- The Fluid Structure Interaction is the interaction of a movable or deformable structure with an internal or a surrounding fluid flow. To tackle those kind of problems efficient numerical approaches are needed, based on the coupling of computational fluid dynamics and computational structural dynamics.
- The proposed FSI modal approach allows the adaptation of the shape of the deformable structure according to modes superposition during the advancement of the computation, lowering the computational cost by eliminating the bottleneck represented by the complex data mapping between the two solvers.
- The modal superposition FSI method will be implemented to investigate an industrial problem: the vortex induced vibration of a thermowell, cylindrical fittings used to protect temperature sensors installed in industrial processes, immersed in a fluid flow.

Vortex shedding phenomenon

Vortex shedding is an oscillating flow that occurs when a fluid flows past a bluff body at specific Reynolds number. In this flow vortices detach periodically and alternately from the body generating a Von Kármán vortex street.

$$Re = \frac{\rho U D}{\mu}$$

Re<4 → Creeping laminar flow

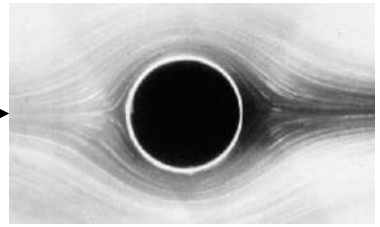

5<*Re*<49 → Symmetric and steady wake

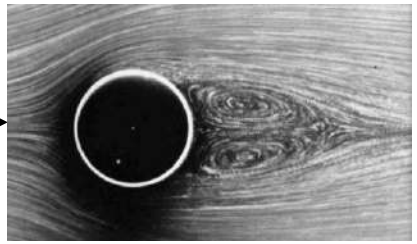

49<*Re*<140-194 → Laminar vortex shedding

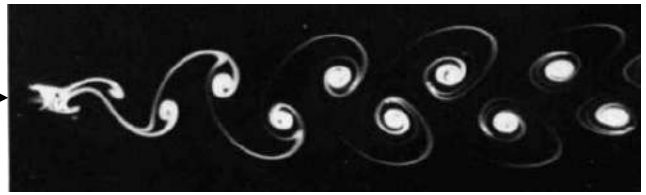

1000<*Re*<200000 → Sub-critical regime

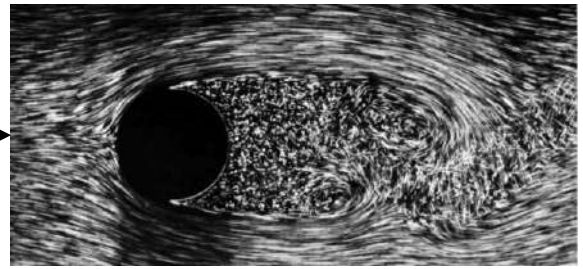

To describe the vortex shedding frequency, the Strouhal number is introduced: $St = \frac{fL}{U}$

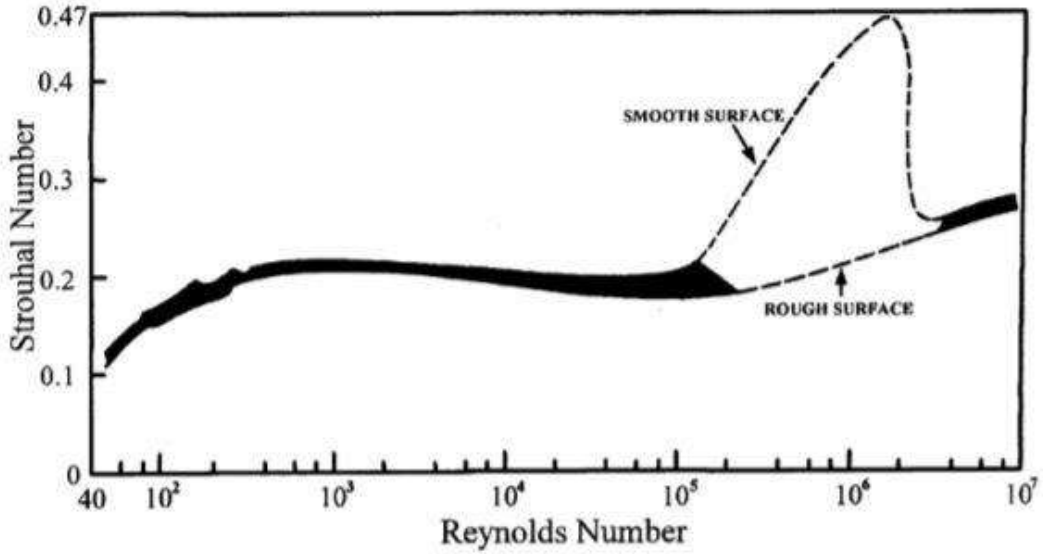

The alternating detachment of vortices provokes alternating low pressure zone on each side of the cylinder, which exerts an unsteady cross-flow force with the same frequency as the vortex shedding and a streamwise unsteady force with a frequency about doubled.

If the Strouhal frequency approaches a natural frequency of the flexible body around which the vortex shedding appears, an oscillatory response may occur ⇒ lock-in.

Theoretical background

The proposed FSI method is based on the modal theory: the structural deformation can be thought as a linear superimposition of the modal shapes of the body itself, so that by importing the modal shapes in the CFD solver with a mesh morphing tool, the numerical grid can be made implicitly elastic.

Modal analysis:

In structural dynamics a modal analysis aims to calculate the structural modes, each one defined by a modal frequency and characterized by a modal shape: the modal frequencies are the frequencies at which the structure would tend to naturally vibrate when subjected to a disturbance and the mode shapes are the patterns of the motions of the structure at each natural frequency.

Second order differential system of equation of motion for a generic n-degrees-of-freedom system:

$$[\boldsymbol{M}]\ddot{\boldsymbol{y}} + [\boldsymbol{C}]\dot{\boldsymbol{y}} + [\boldsymbol{K}]\boldsymbol{y} = \boldsymbol{Q}$$

Hypothesis: conservative system, synchronous motion ⇒ eigenvalue problem:

$$[\boldsymbol{K}]\boldsymbol{v} = \omega_n^2[\boldsymbol{M}]\boldsymbol{v}$$

Mass normalization:

$$\boldsymbol{v}_i^T[\boldsymbol{M}]\boldsymbol{v}_i = 1$$

$$\boldsymbol{v}_i^T[\boldsymbol{K}]\boldsymbol{v}_i = \omega_{n,i}^2$$

Modal coordinates formulation:

Eigenvectors are orthogonal with respect to both stiffness and mass matrices:

$$\boldsymbol{v}_j^T[\boldsymbol{M}]\boldsymbol{v}_i = 0 \qquad i \neq j$$

$$\boldsymbol{v}_j^T[\boldsymbol{K}]\boldsymbol{v}_i = 0 \qquad i \neq j$$

⇒ eigenvectors are linearly independent ⇒ new reference system ⇒ modal matrix:

$$[\boldsymbol{v}] = \left[\boldsymbol{v}_1 \boldsymbol{v}_2 \ldots \boldsymbol{v}_n\right]$$

Modal vector coordinates:

$$\boldsymbol{q} = [\boldsymbol{v}]^{-1}\boldsymbol{y}$$

$$\Downarrow$$

$$\ddot{q}_i + 2\varsigma_i\omega_{n,i}\dot{q}_i + \omega_{n,i}^2 q_i = \frac{F_i(t)}{m_{ii}}$$

Each mode acts as a single-degree-of-freedom dynamic system and the overall system response can be calculated as a linear superimposition of each mode response.

Unsteady FSI using modal superposition:

Hypothesis: modal force *F* can be considered constant within every time-step of integration

$$\Downarrow$$

$$q(t) = e^{-\varsigma\omega_n t}\left[q_0\cos(\omega_d t) + \frac{\dot{q}_0 + \varsigma\omega_n q_0}{\omega_d}\sin(\omega_d t)\right] +$$

$$+e^{-\varsigma\omega_n t}\left\{\frac{F}{\omega_d}\left[\frac{4\omega_d}{\varsigma^2\omega_n^2 + 4\omega_d^2} - e^{-\varsigma\omega_n t}\frac{2\varsigma\omega_n\sin(\omega_d t) + 4\omega_d\cos(\omega_d t)}{\varsigma^2\omega_n^2 + 4\omega_d^2}\right]\right\}$$

$$\Downarrow$$

$$\boldsymbol{y} = \sum_{i=1}^{\boldsymbol{n}} \boldsymbol{v_i} q_i$$

Not all the frequencies are excited ⇒ modes truncation.

Modal FSI workflow:

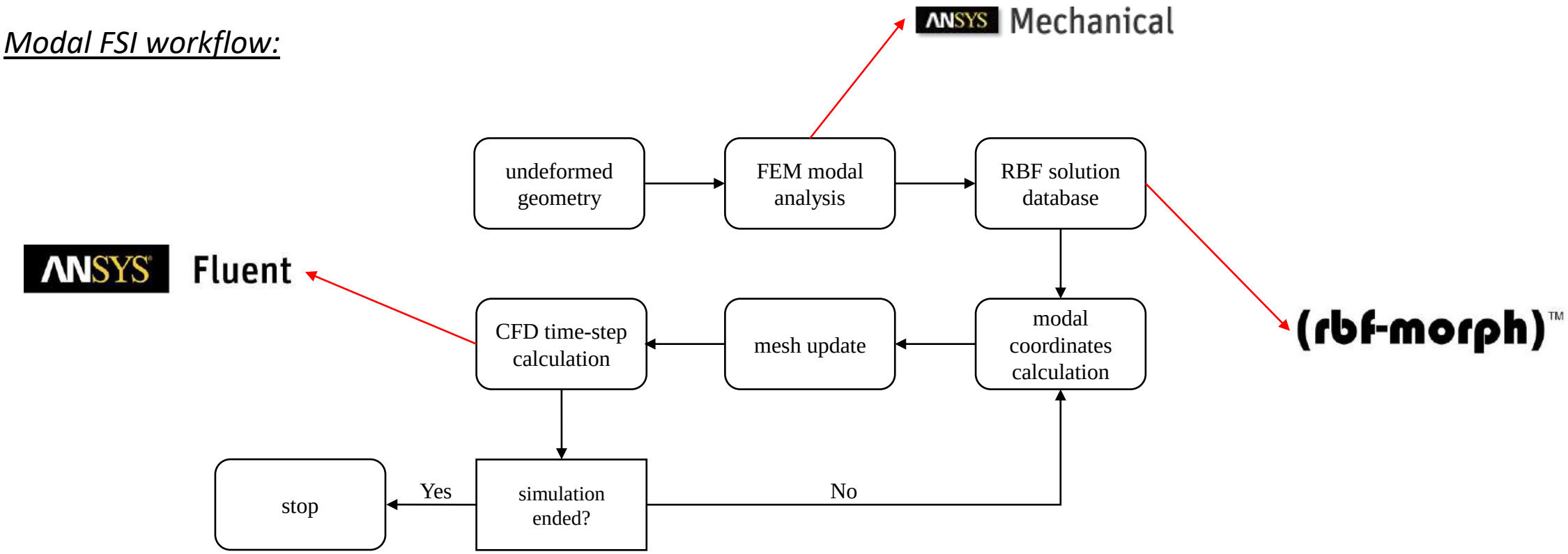

To speed up the mesh morphing step, the deformations associated with each modal shape are stored in memory. This is possible because the mesh deformations are obtained by linearly superimposing the action of each modal shape amplified by its modal coordinate:

$$\boldsymbol{x}_{CFD}(t) = \boldsymbol{x}_{CFD_0} + \sum_{i=0}^{k} q_{\boldsymbol{i}}(t)\Delta\mathbf{x}_i$$

Two-dimensional CFD analysis

Before proceeding with the three-dimensional FSI analysis, a preliminary two-dimensional study was conducted in order to define an adequate CFD setup able to capture the vortex shedding phenomenon.

The testing conditions chosen for the 2-D analysis consist of an air flow at *Re*=50000, inside the sub-critical regime of the vortex shedding phenomenon, which is characterized by a very large spectrum of applications, including the one analysed in this work.

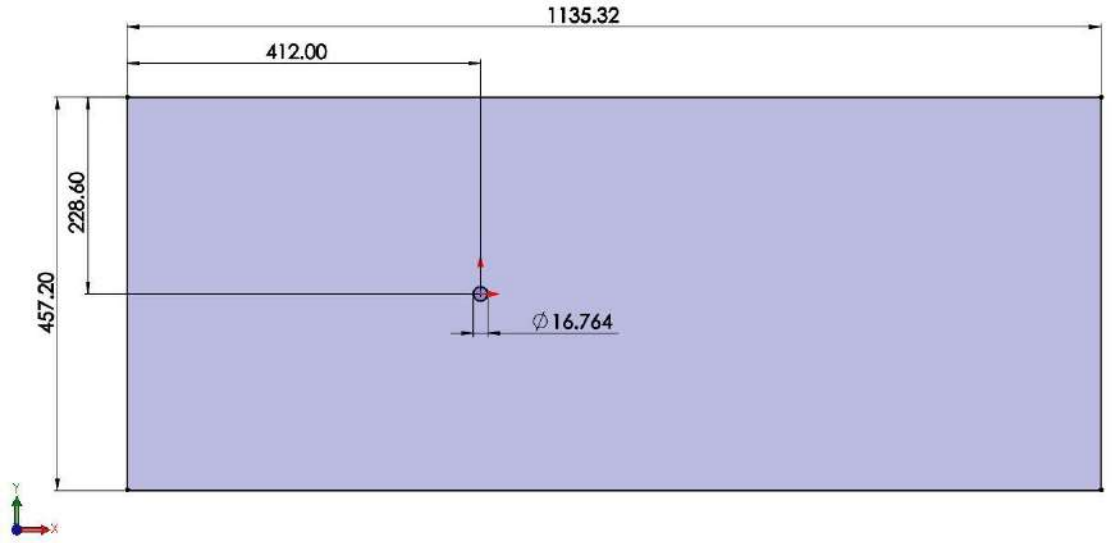

2-D computational grid:

The geometry has been discretized into a computational domain through ANSYS® ICEM CFD™. The obtained mesh is structured, multiblock and composed of quadrilaterals.

Key features: $y^+<1$ for the first row of cells near the cylinder, 1.2 growth factor after the first row, refinement in the wake, 110722 cells.

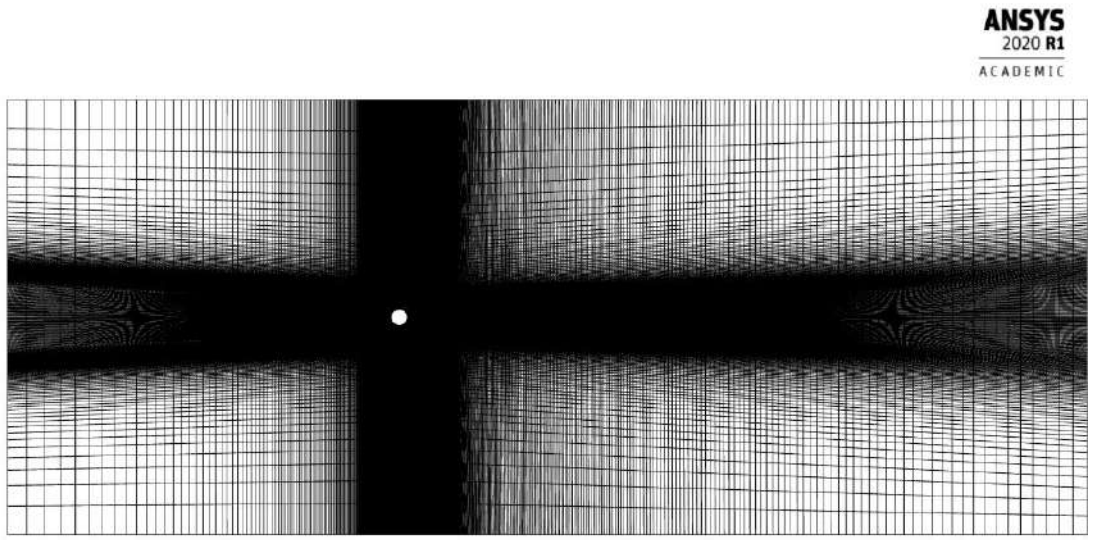

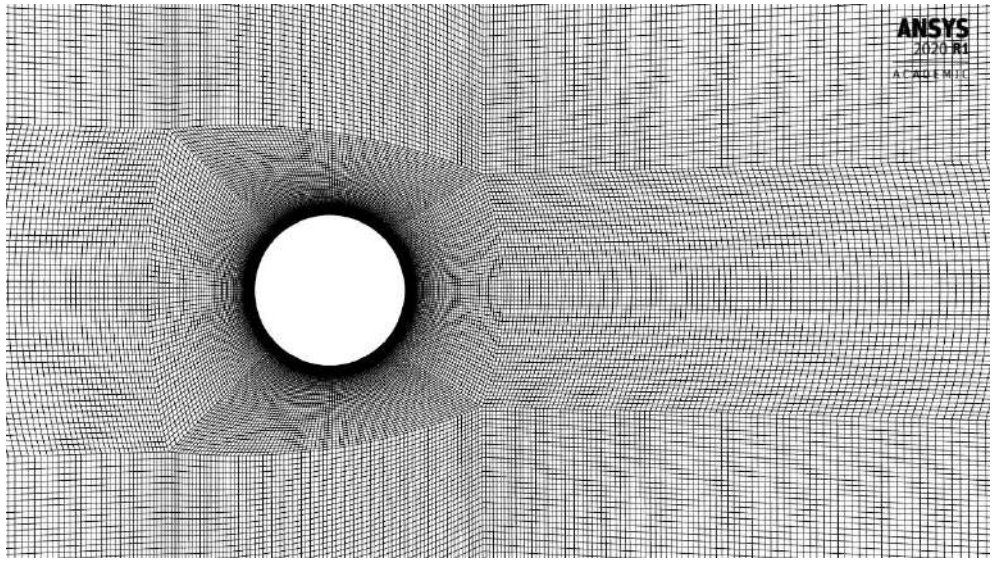

Mesh quality evaluation: 0.782 minimum orthogonal quality, 0.218 maximum cell squish index.

2-D CFD setup:

The 2-D grid has been extruded in the third dimension for one meter, keeping only one cell in the thickness.

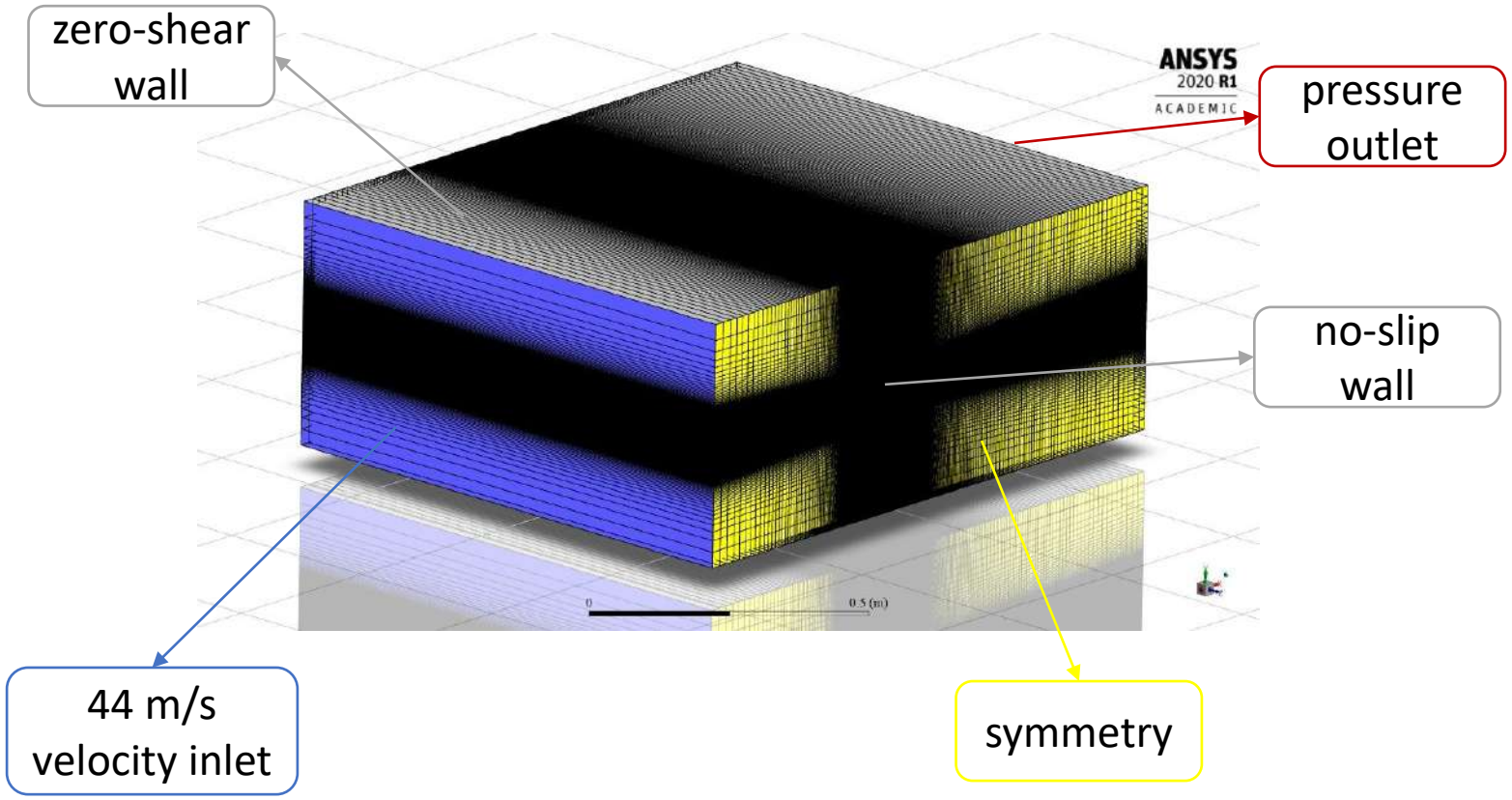

Key features:

- Air density: 1.225 kg/m^3;
- Air viscosity: 1.7894·10^{-5} kg/(m·s);
- Mach number: 0.12;
- Pressure-based solver;
- Constant density;
- URANS with SST k-ω;
- SIMPLE pressure-velocity coupling;
- Second order scheme for pressure;
- Second order upwind scheme for momentum and turbulence parameters;
- Lest squares cell based scheme for gradient;
- First order implicit transient formulation.

2-D analysis results:

Time-step size and number of internal iterations are the main parameters influencing the results of the simulations in terms of vortex shedding phenomenology and evolution of the fluid forces acting on the cylinder ⇒ convergence study.

Time-step size [s]	Number of internal iterations
$2 \cdot 10^{-4}$	20
$1 \cdot 10^{-4}$	20
$7.5 \cdot 10^{-5}$	30
$5 \cdot 10^{-5}$	30
$2.5 \cdot 10^{-5}$	30
$1 \cdot 10^{-5}$	30
$7.5 \cdot 10^{-6}$	30
$5 \cdot 10^{-6}$	30
$2.5 \cdot 10^{-6}$	30
$1 \cdot 10^{-6}$	30

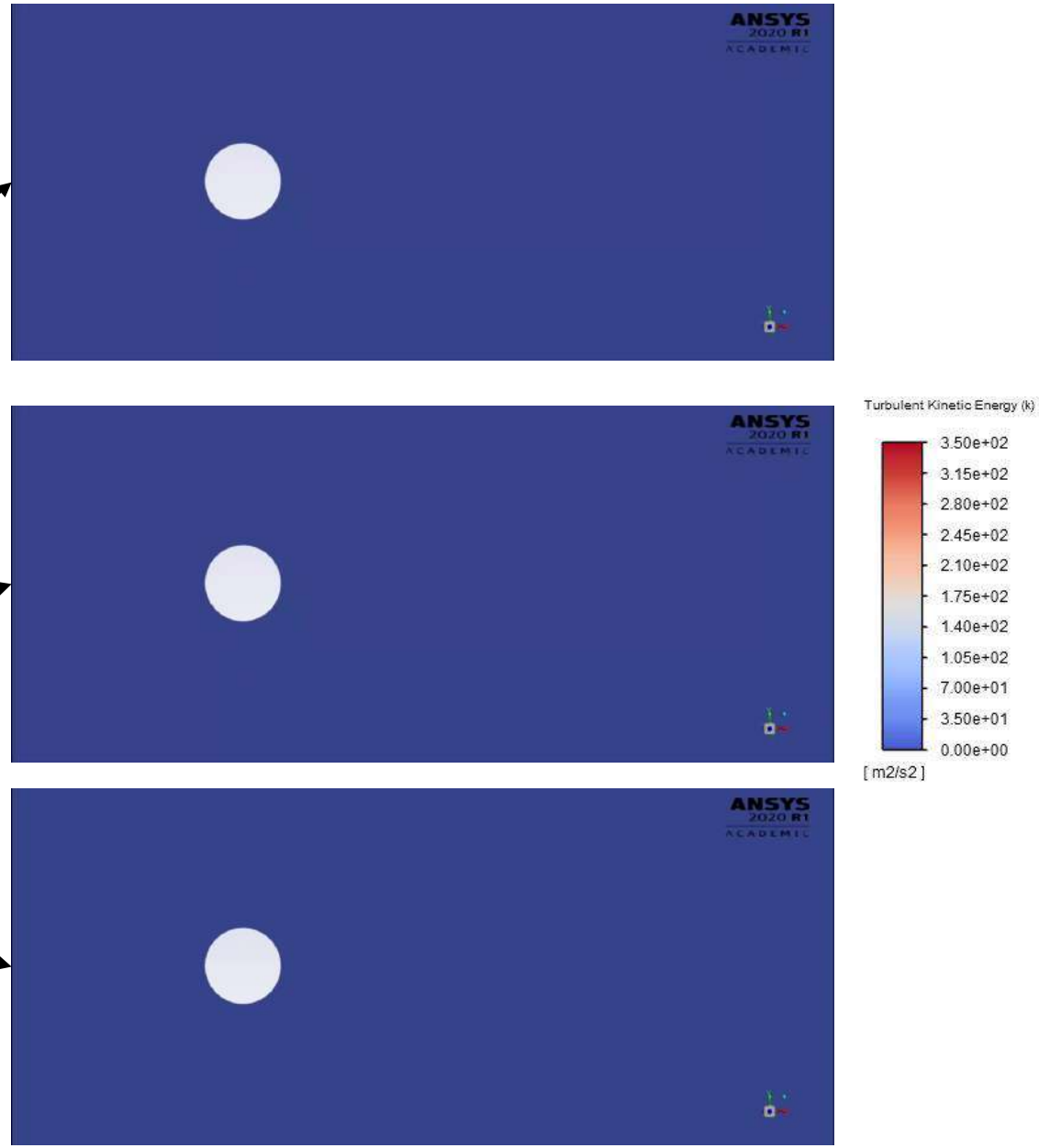

By lowering the time-step size under $1 \cdot 10^{-5}$ s, the dynamic steady state is more or less the same.

Evolution of the drag and the lift coefficients with a time-step size of $1 \cdot 10^{-5}$ s:

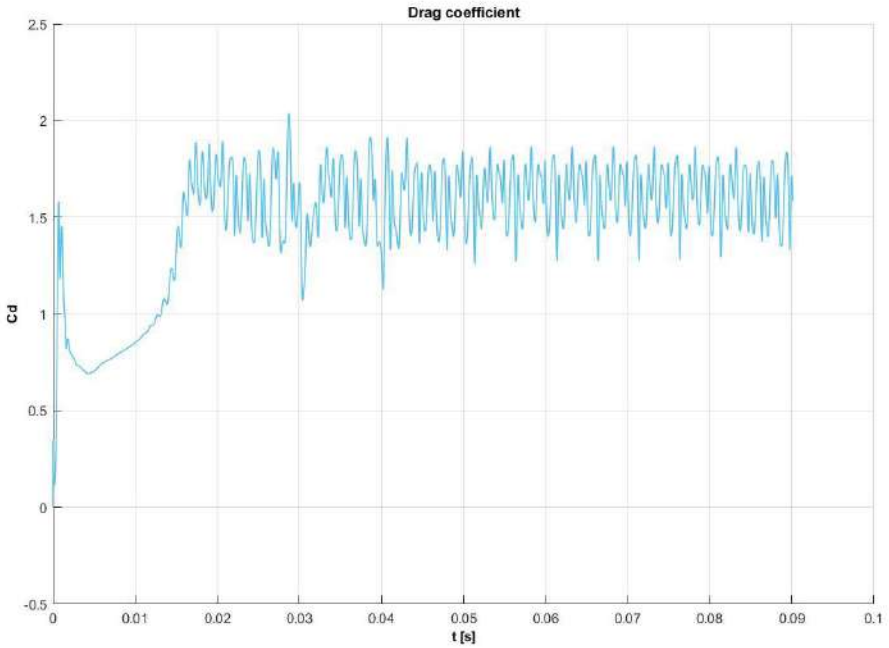

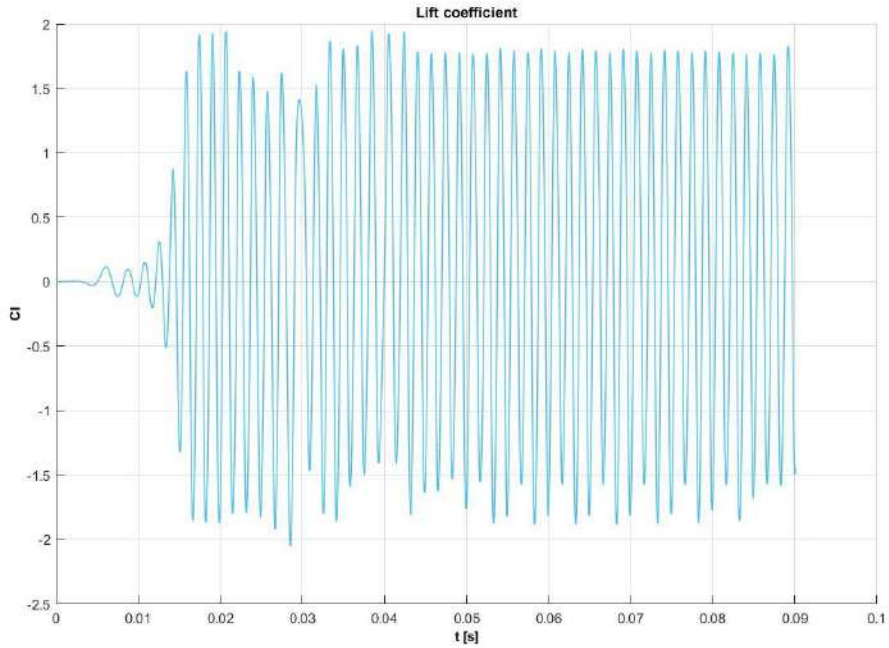

Frequency analysis:

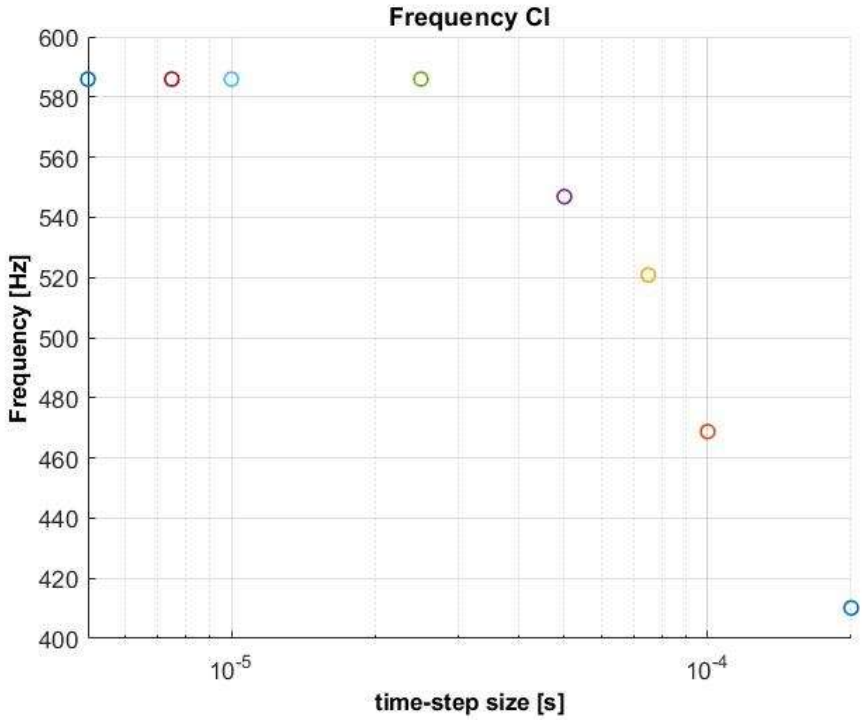

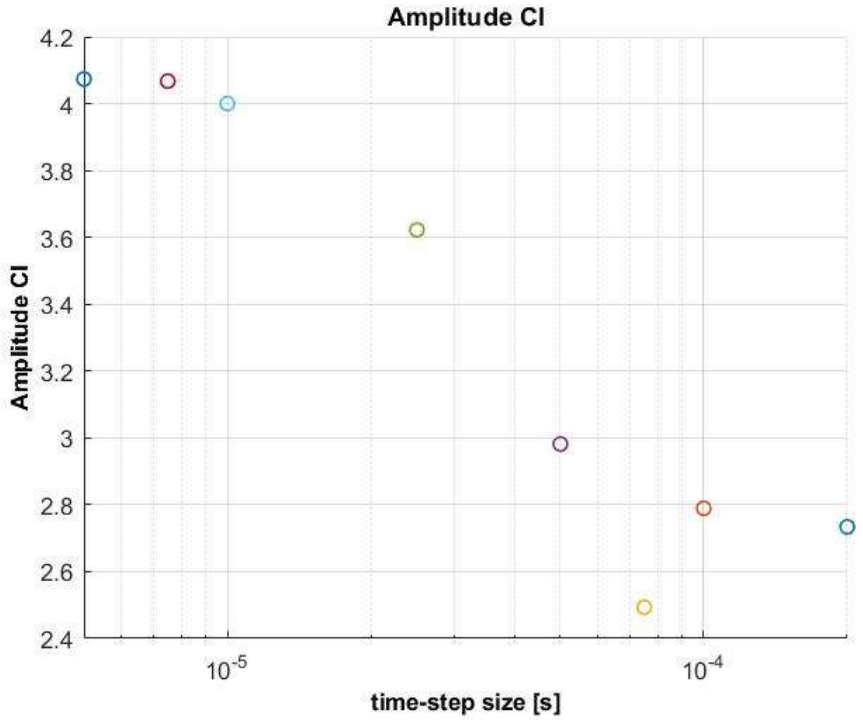

At the considered *Re* the expected *St* is about 0.2 ⇒ vortex shedding frequency of 524.93 Hz. The obtained shedding frequency, for a time-step size of 10^{-5} s or lower, is 585.94 Hz ⇒ -11.62% error due to: RANS formulation for an highly unsteady phenomenon, 2-D analysis for an highly three-dimensional phenomenon.

Nevertheless the proposed CFD setup was able to solve with acceptable accuracy the shedding phenomenon both from a qualitative and a quantitative point of view ⇒ both the CFD setup and the grid features were considered reliable and applied to the three-dimensional FSI study.

Vortex induced vibration analysis

Experimental investigation:

The investigated industrial problem is about the vortex induced vibration of a thermowell immersed in a fluid flow. The case study taken as a reference is presented in a video loaded on the website of Emerson Electric Co., the multinational corporation that owns Rosemount Inc., the manufacturer of the studied thermowell.

The aim of the experiment was to evaluate the flow induced vibrations of two possible thermowell designs: the traditional one and the twisted square one.

The two tested thermowells, both with 470.219 mm in length, were equipped with accelerometers in the tip and immersed in a water flow loop evolving inside a 152.4 mm diameter pipe. To evaluate the flow induced vibrations of the two thermowells, the water velocity ranged from 0 m/s to 8.5 m/s.

Results:

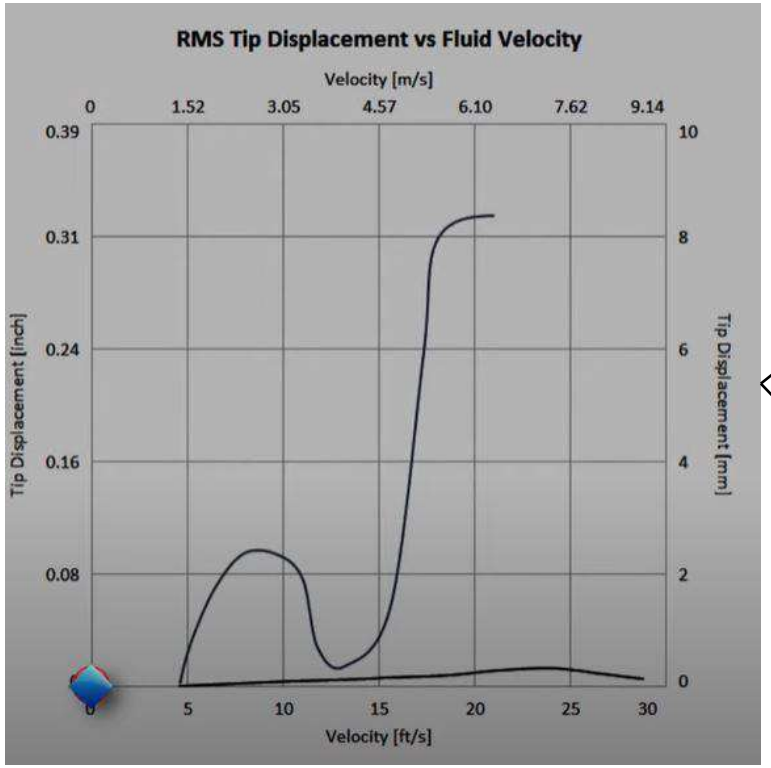

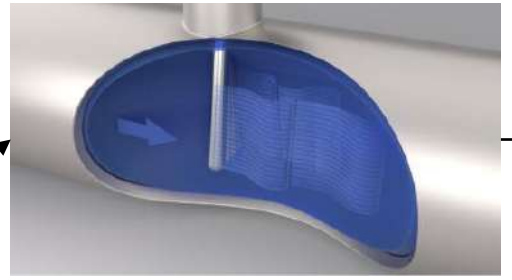

Cylindrical thermowell

Two lock-in regions:

- In-line vibration: 2.33 mm maximum rms tip displacement at 2.44 m/s fluid velocity;
- Transverse vibration: 8.3mm maximum rms tip displacement at 6.4 m/s fluid velocity.

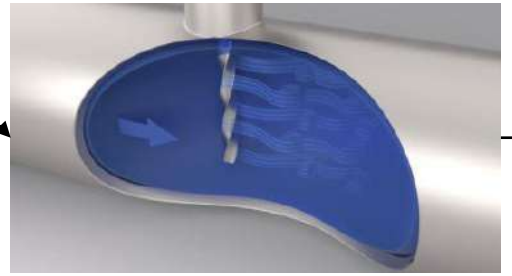

Twisted square thermowell

No lock-in regions.

Geometry:

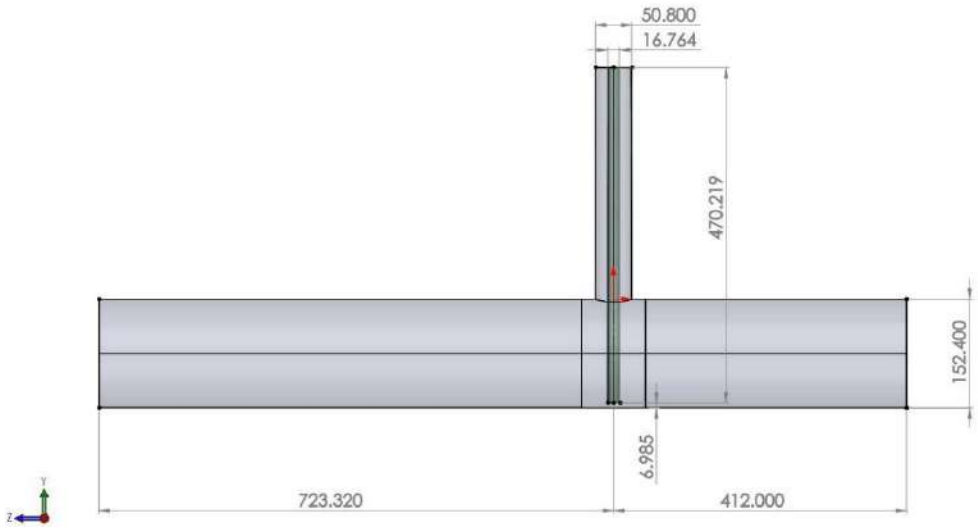

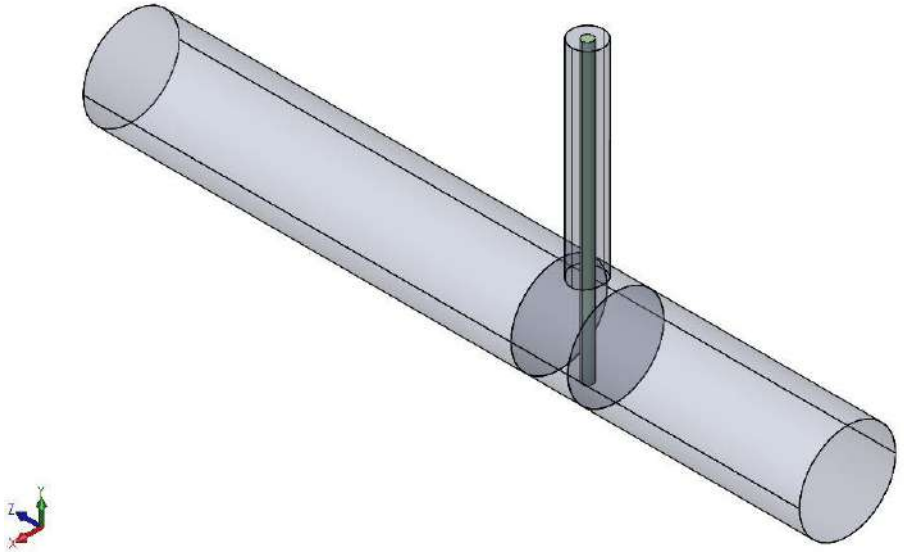

Modal analysis:

The first step needed to setup a FSI analysis based on the modal superposition method is to carry out a modal analysis of the deformable structure.

Material: 304/304L dual rated steel with a density of 7750 kg/m3, a Young's modulus of 200 GPa and a Poisson's ratio of 0.3.

FEM setup:

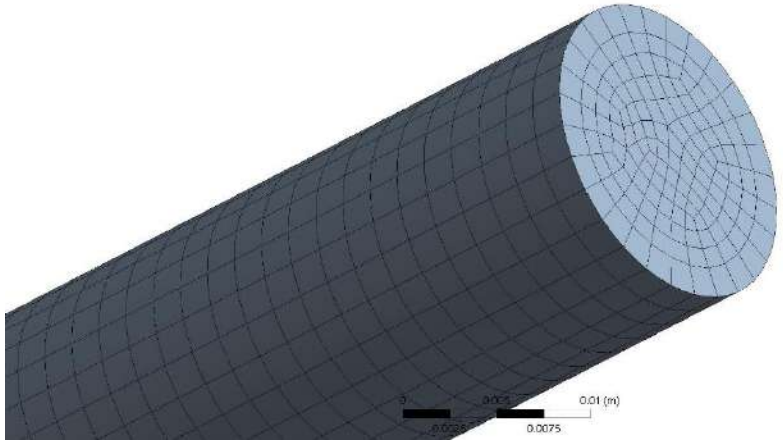

Key features:

- Uniform mesh to correctly represent the distribution of mass and stiffness;
- 2 mm element size;
- 34456 20-noded hexahedrons for a total of 148675 nodes;
- Cantilever beam;
- Neither damping nor pre-stress
- 12 modes extracted, but only the first 6 are employed in the FSI study.

Convergence study:

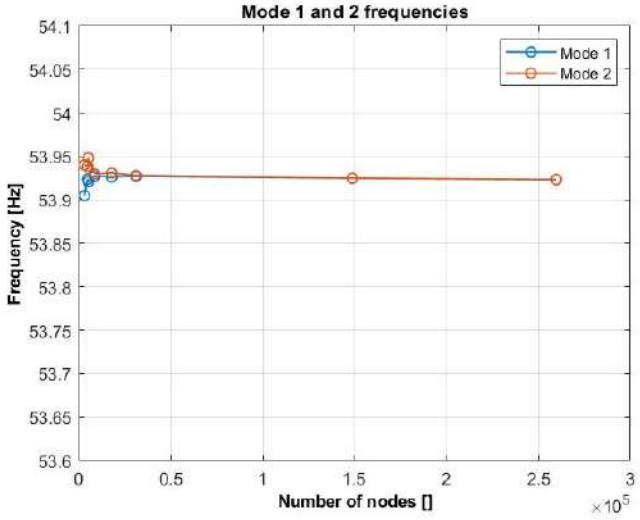

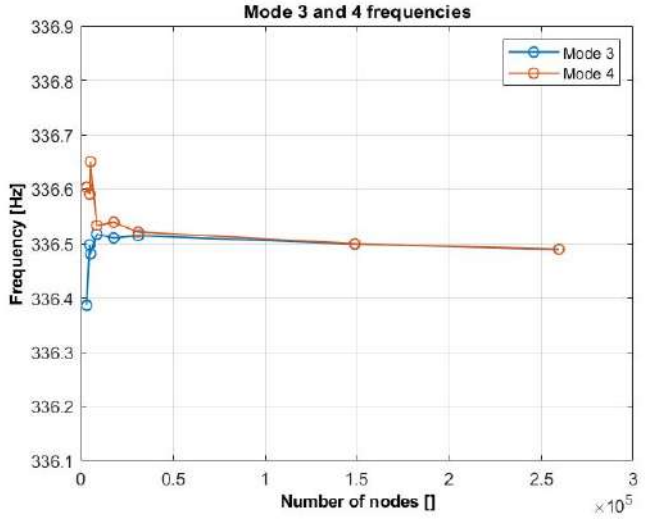

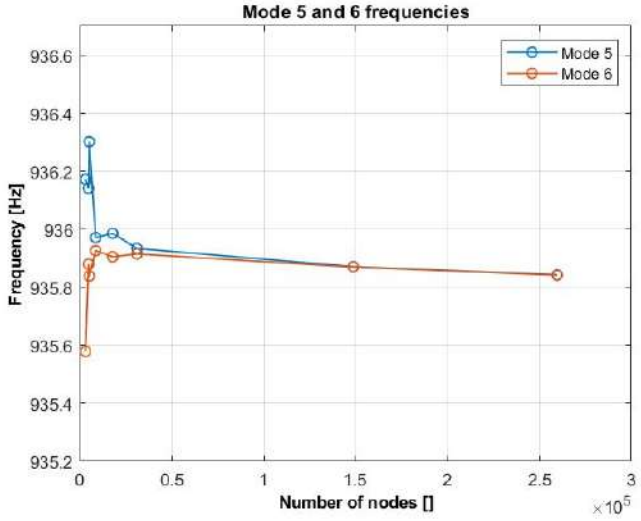

Modal shapes:

Algebraic multiplicity of two of the bending modes ⇒ six computed natural modes, correspond to only three distinct bending modes.

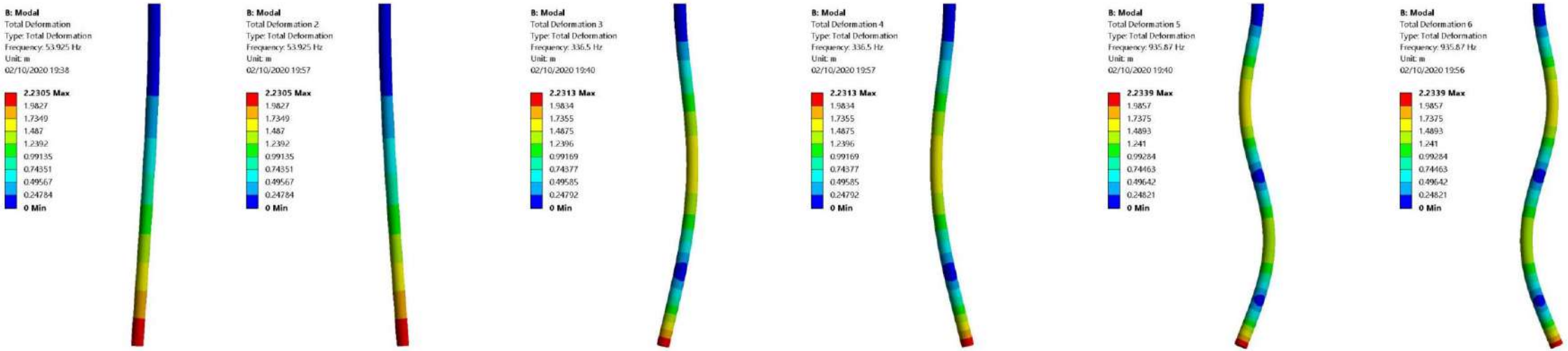

Analytical results: $\omega_{n,i} = \alpha_i^2 \sqrt{\frac{EI_B}{\rho A_B L_B^4}} \quad i = 1,2,3$ ⇨

Mode	Analytical natural frequency [Hz]	FEM natural frequency [Hz]	Relative error [%]
1	53.883	53.925	-0.0779
2	337.681	336.499	0.34999
3	945.523	935.872	1.0207

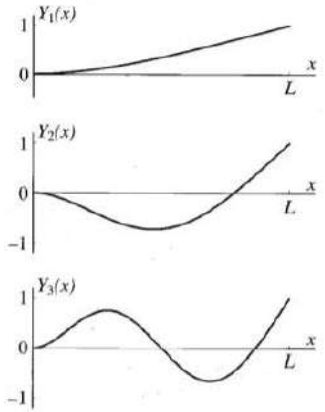

RBF solutions setup:

Two-step technique for each natural mode.

First step: loads the previously generated .pts file corresponding to the considered modal shape (first six).

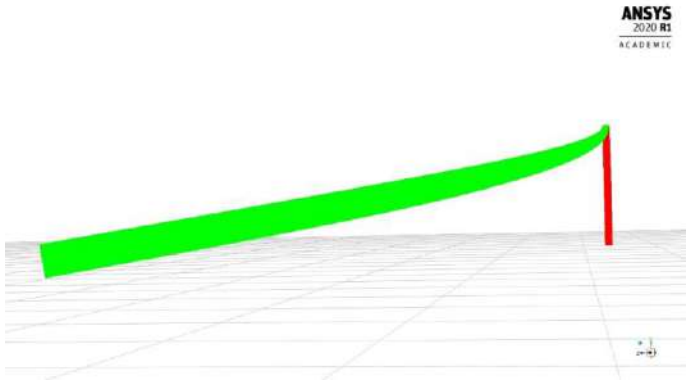

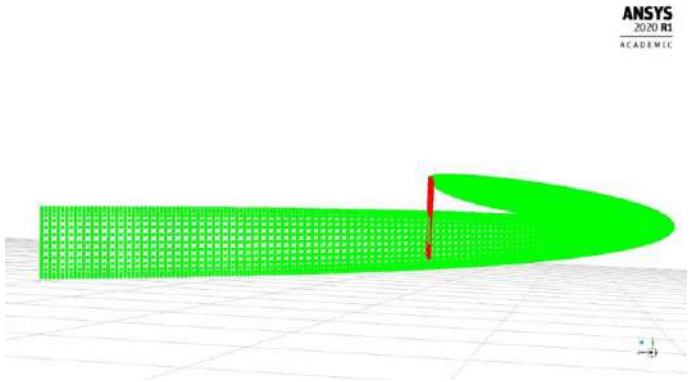

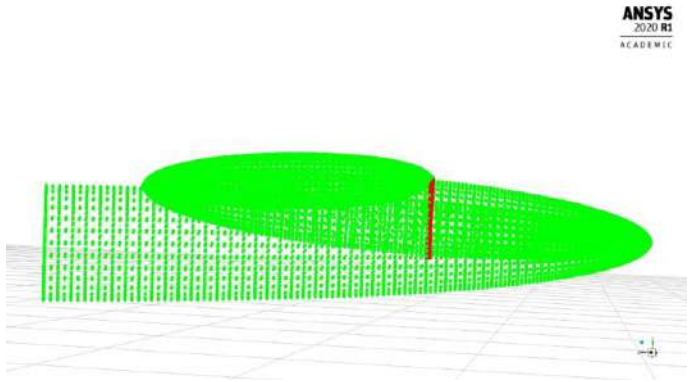

Second step: the first RBF solution, amplified with a factor of 0.001 , is imposed as a motion law to the thermowell surface and a domain encapsulation is introduced to delimit the action of the morphing.

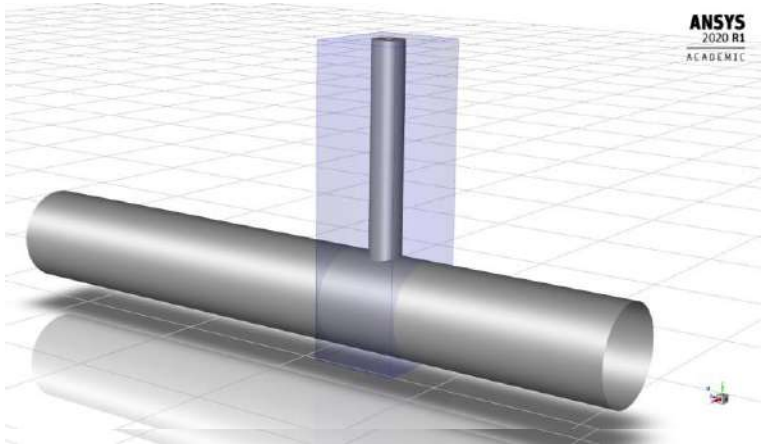

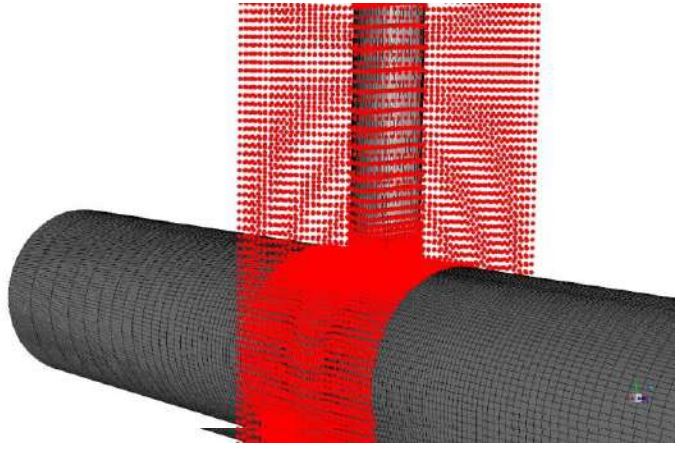

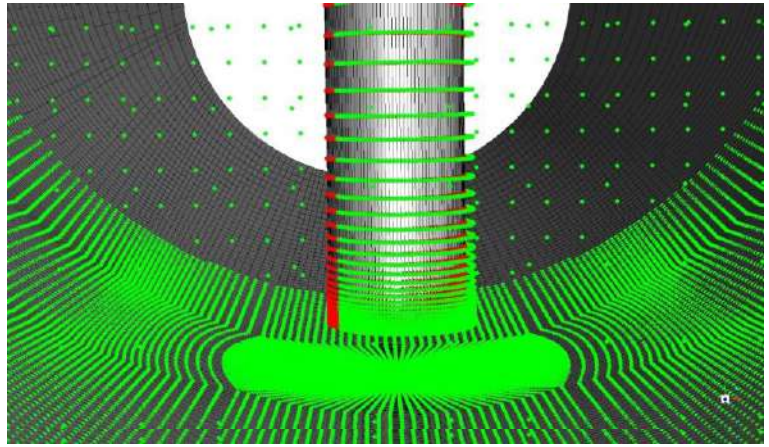

Corrective RBF solutions:

Proximity of the tip of the thermowell to the boundary of the simulation volume (fixed) ⇒ high volume mesh distortion.

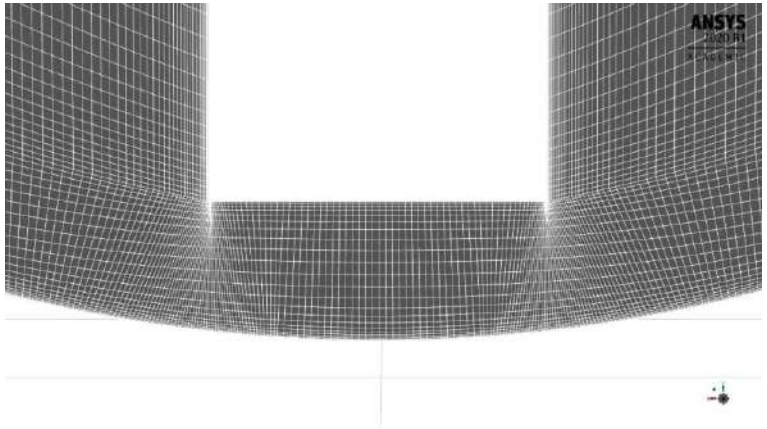

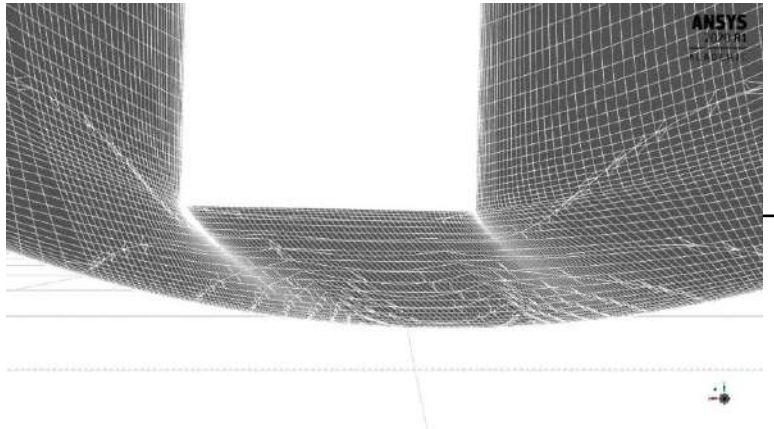

Quality evaluation:

- minimum orthogonal quality: 0.016
- maximum cell squish index: 0.984

Three corrective solutions: shadow area rotation, shadow area translation, STL-target-derived.

Shadow area management: the shadow area is the portion of the duct surface linked to the tip of the thermowell through the structured mesh ⇒ to avoid the high mesh distortion, the surface nodes contained in this area had to follow the tip of the thermowell during the morphing action ⇒ rotation around the pipe axis and translation in the direction of the axis.

Shadow area rotation:

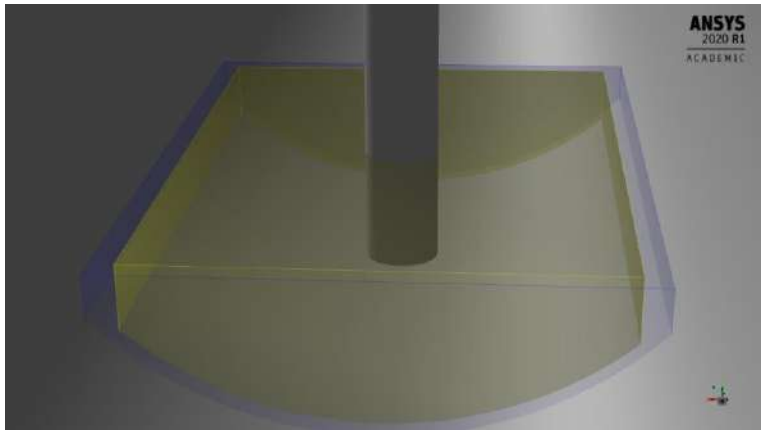

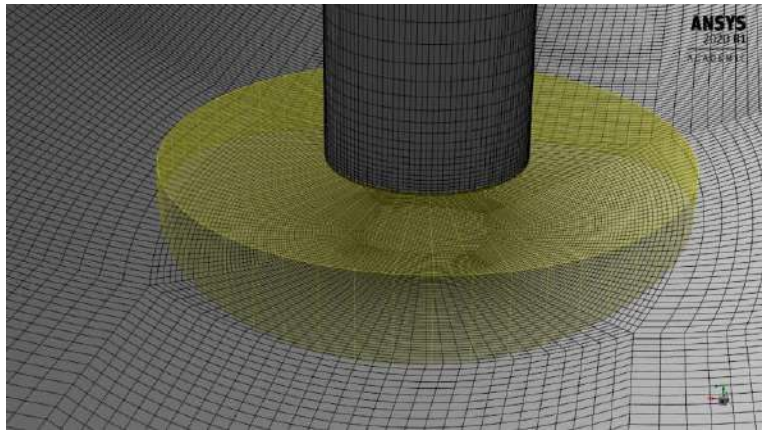

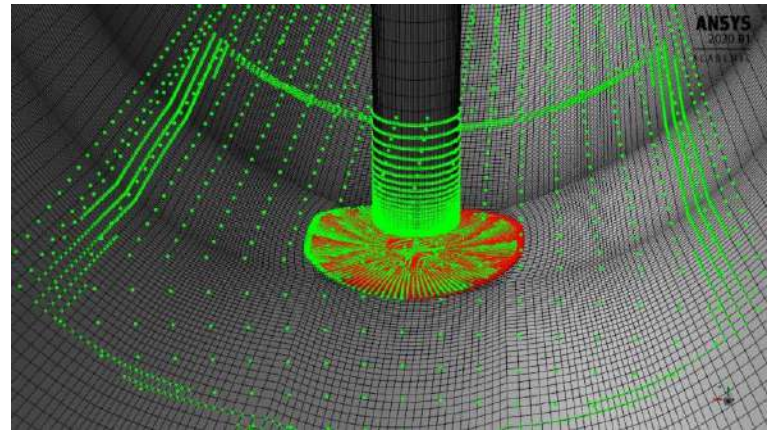

STL-target-derived corrections: the absence of source points on the rest of the duct surface caused the loss of direct control on its morphing ⇒ distortion of the cylindrical surface ⇒ STL-target motion:

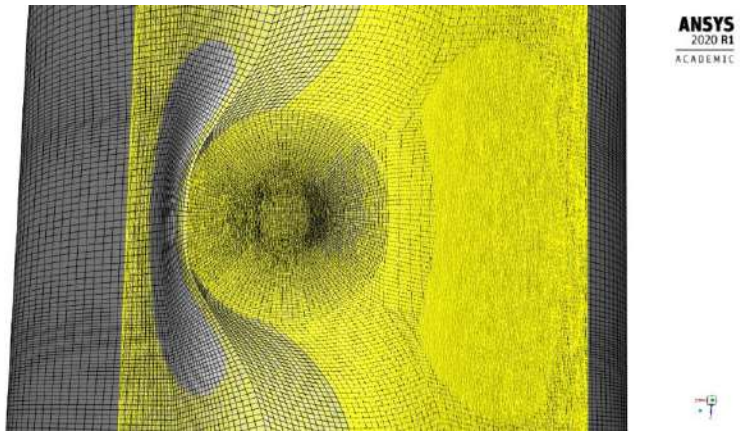

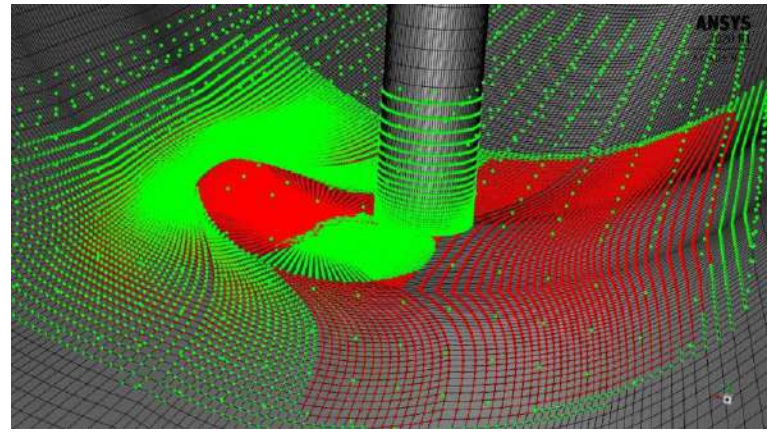

If the rotation of the shadow area is applied with an amplification factor lower than the maximum one (15°, used to build the STL-target solution) there is no way in which the implementation of a proportionally amplified STL-target solution could recover the cylindricity of the duct, due to the wrong choice of the starting points ⇒ the recovery solution has to be defined starting from the undeformed surface.

Three meshes are available: the starting one, the distorted one and the recovered one ⇒ using the domain node number the position of each node in the domain encapsulation was tracked in the three meshes ⇒ a new .pts file was written in which the source points were the nodes extracted from the starting surface mesh (inside the domain encapsulation) and their displacement was calculated as the difference between their corresponding position in the recovered mesh and in the distorted mesh ⇒ recovery solution defined starting from the undeformed mesh.

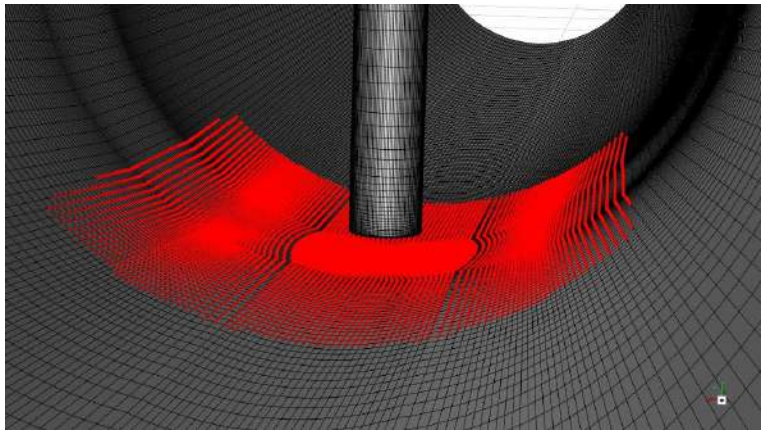

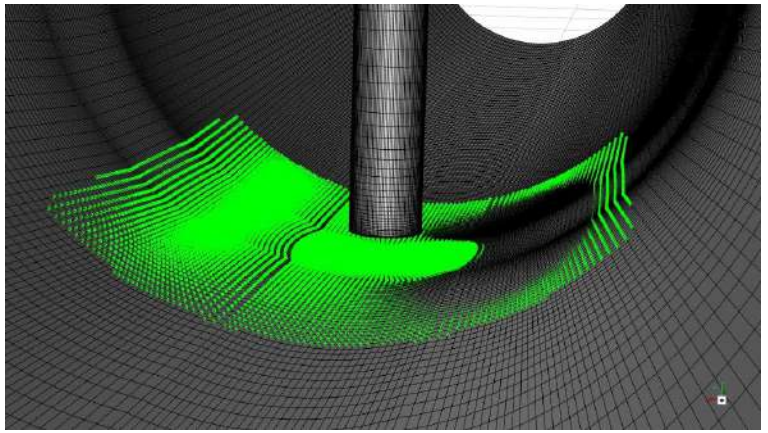

If the rotation of the shadow area is applied with an amplification factor lower than 15, the cylindricity of the duct can be recovered applying this STL-target-derived solution with a proportional amplification factor

If the shadow rotation is applied with a negative amplification factor this corrective solution is no longer viable ⇒ a similar corrective solution was built, following the same steps but starting from a -15° maximum rotation.

Effects of the corrective solutions:

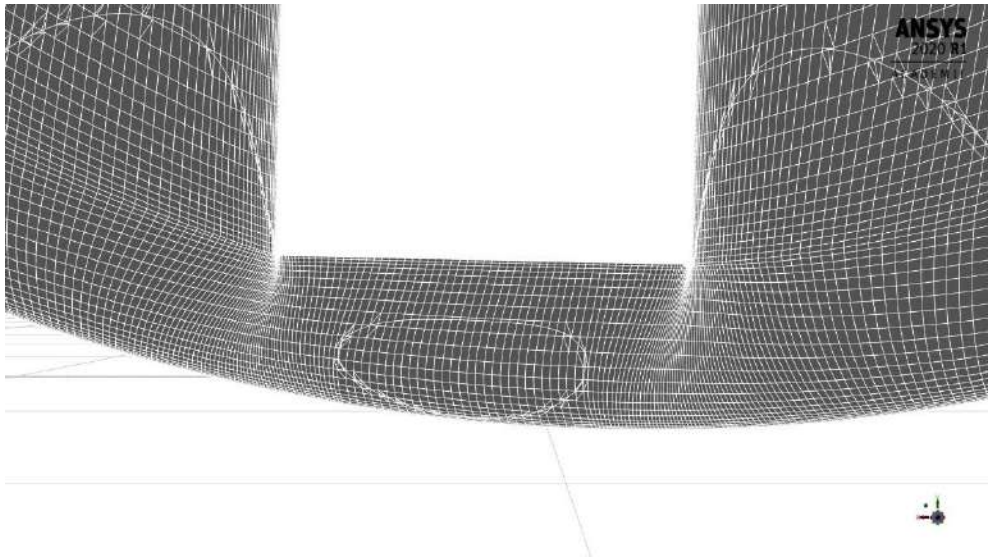

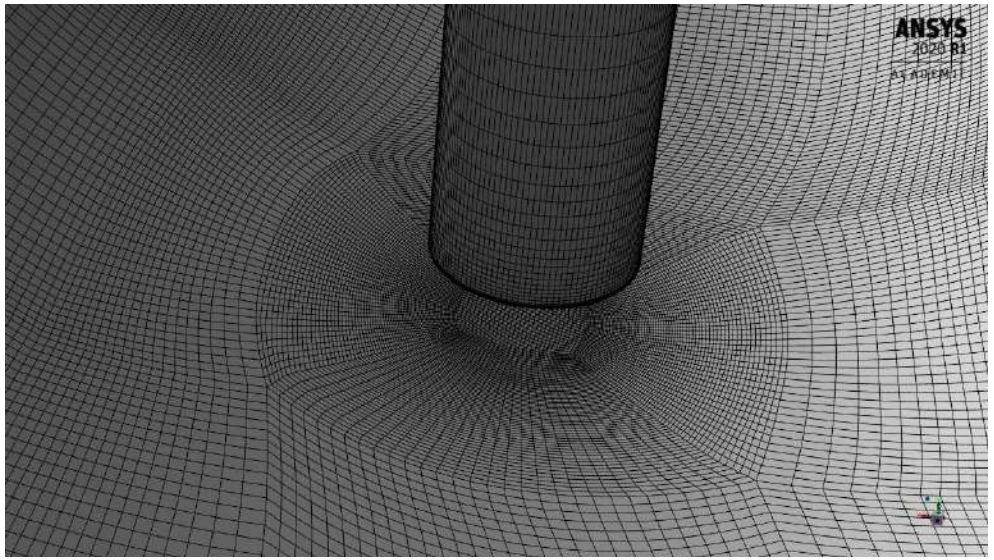

- Improvement in morphing quality (lower mesh distortion);
- Preservation of the cylindricity of the duct;
- Correct positioning of the shadow area.

3-D computational grid:

The geometry has been discretized into a computational domain through ANSYS® ICEM CFD™ using the setup validated in the 2-D analysis. The obtained mesh is structured, multiblock and composed of hexahedrons.

Key features: $y^+<1$ for the first row of cells near the walls, 1.2 growth factor after the first row, refinement in the wake, 3158640 hexahedral cells.

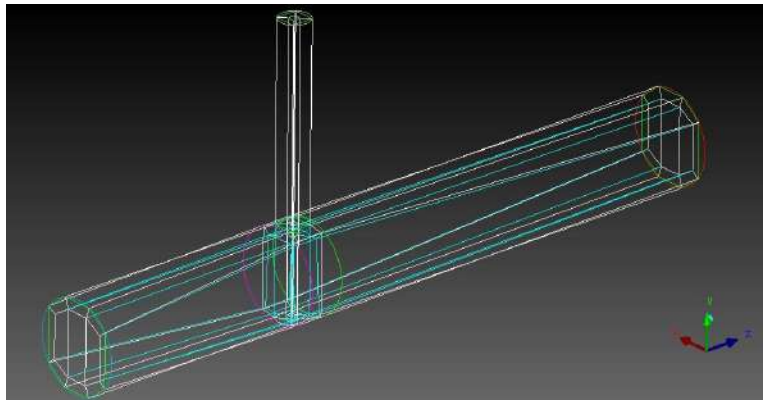

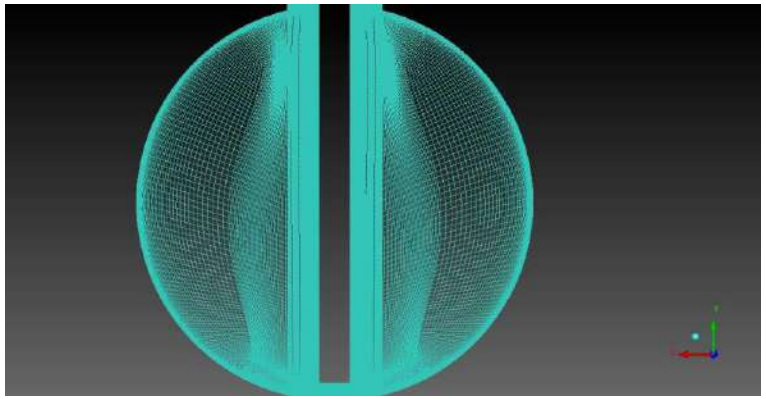

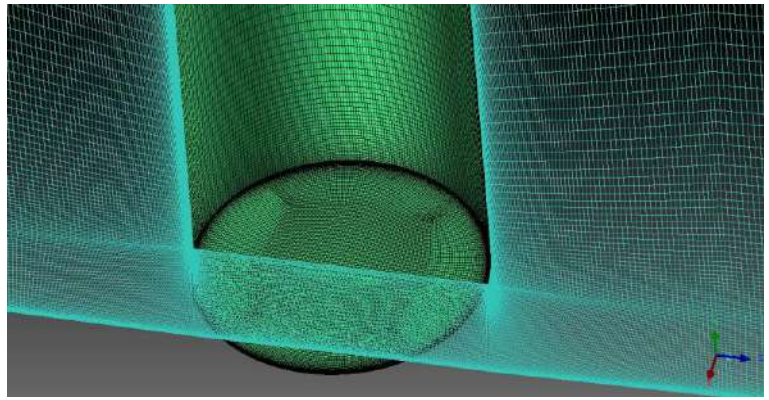

Mesh quality evaluation:

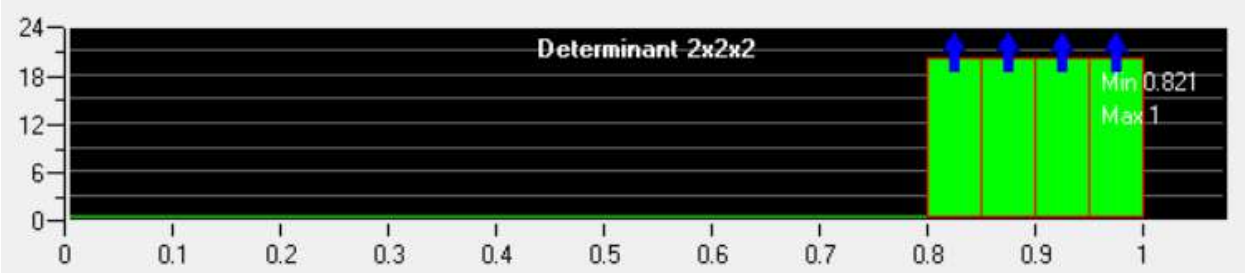

CFD setup:

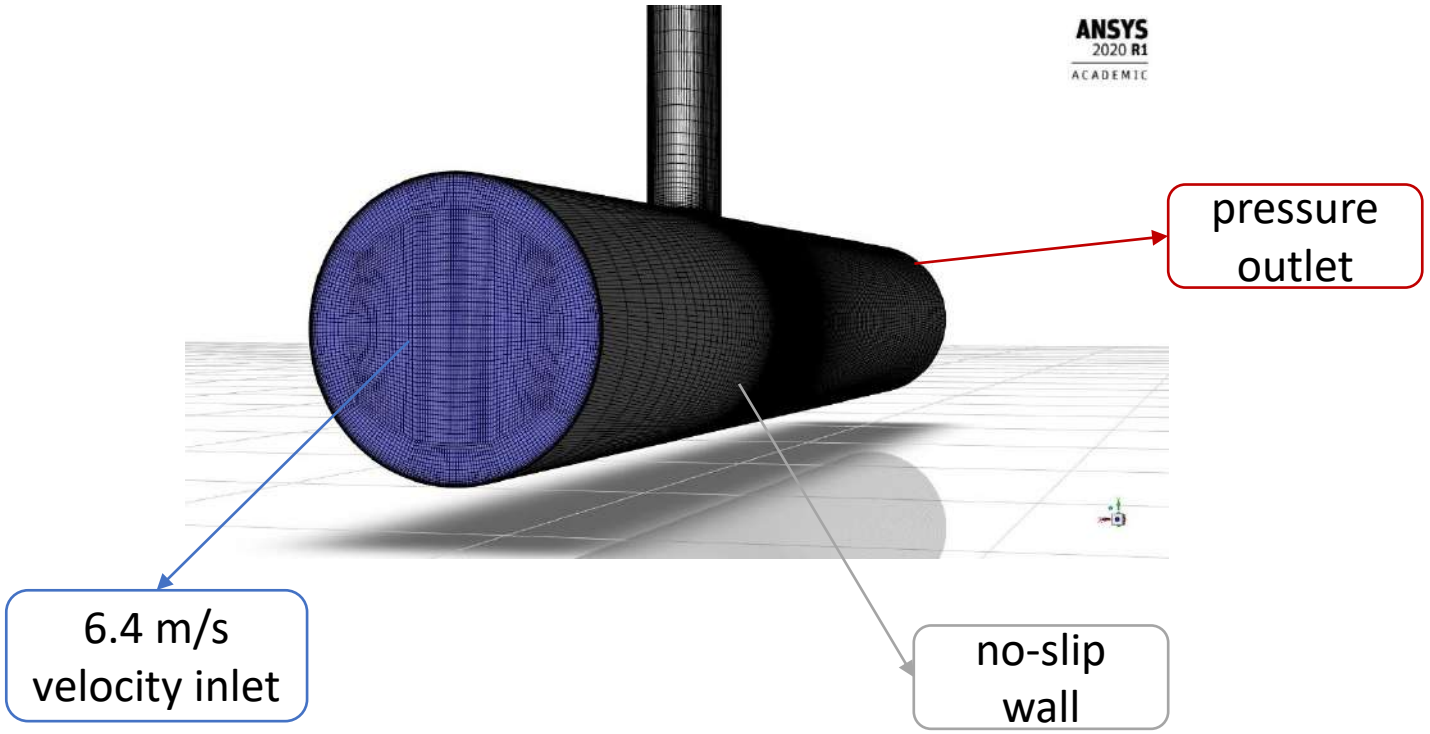

Key features:

- Water density: 998 kg/m^3;
- Water viscosity: 0.001002 kg/(m·s);
- *Re*: 100000;
- Pressure-based solver;
- Constant density;
- URANS with SST k-ω;
- SIMPLE pressure-velocity coupling;
- Second order scheme for pressure;
- Second order upwind scheme for momentum and turbulence parameters;
- Lest squares cell based scheme for gradient;
- First order implicit transient formulation;
- Time-step size: 10^{-4} s;
- Computer-controlled convergence criterion: 10^{-5} residual of the continuity equation.

FSI setup:

1. Parameters definition ⇒ morphed surfaces, RBF solutions, frequencies, time-step size, damping ratio;
2. Files loading ⇒ an executable that handles the unsteady FSI analysis and a scheme function that handles the corrective solutions;
3. FSI environment initialization ⇒ the RBF solutions are loaded and stored in memory;
4. Commands setting ⇒ *(shadow_control)* and *(modal-q-update)* executed at the end of each timestep.

***(modal-q-update)*:** calculates the values of the modal forces projecting the nodal forces onto the modal shapes, updates the modal coordinates and applies the mesh morphing over-imposing linearly each solution with respect to the baseline with the associated computed modal coordinate as its amplification factor. To cope with the 0.001 amplification factor applied to the solution of the first step, the modal forces and of the modal coordinates before the morphing are multiplied by 1000.

***(shadow_control)*:** computes and enforces the amplification factors of the corrective solutions in order to keep the shadow area under always under the tip of the thermowell, knowing its displacement in the streamwise and cross-flow direction. To cope with the multiplication by 1000 the amplification factors are divided by 1000.

Damping ratio:

The accuracy of any dynamic solution is dependent on the damping assigned to the model, usually defined as a percentage of the critical damping, also called “damping ratio”.

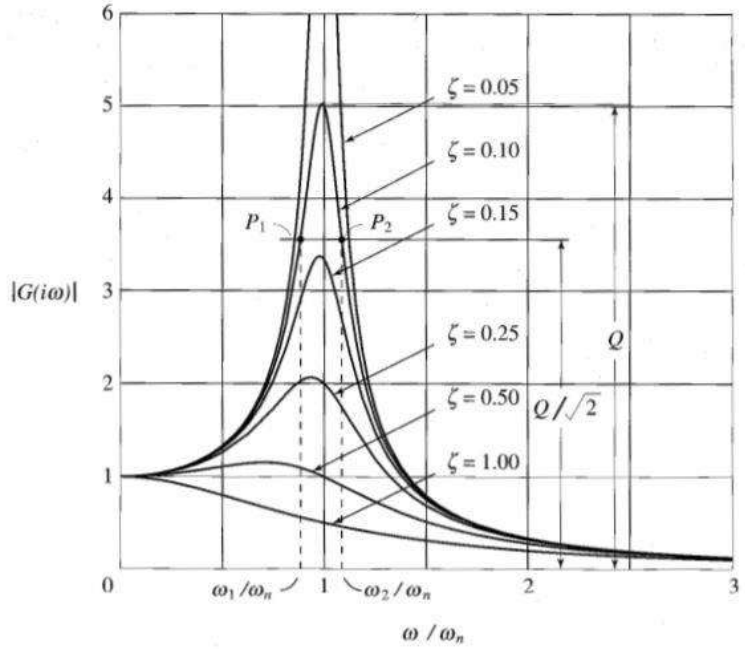

It is a property that should be experimentally measured, not available in the experimental data ⇒ literature guidance:

System	Damping ratio
Metals (in elastic range)	<0.01
Continuous metal structures	0.02 to 0.04
Metal structure with joints	0.03 to 0.07

⇒ Expected damping ratio in the 0.01 to 0.07 range

Parametric study:

The simulations ran on a HPC cluster equipped with 250 GB of RAM and four Intel® Xeon® Gold 6152 CPU, each featuring 22 cores @ 2.1 GHz. Out of the overall 88 cores, 30 were used to run the simulations

Damping ratio	Maximum RMS transverse tip displacement at dynamic steady state [mm]	Relative error [%]
0.01	Not reached	-
0.02	Not reached	-
0.05	6.45	22.3
0.04	8.48	-2.17
0.041	8.304	-0.048

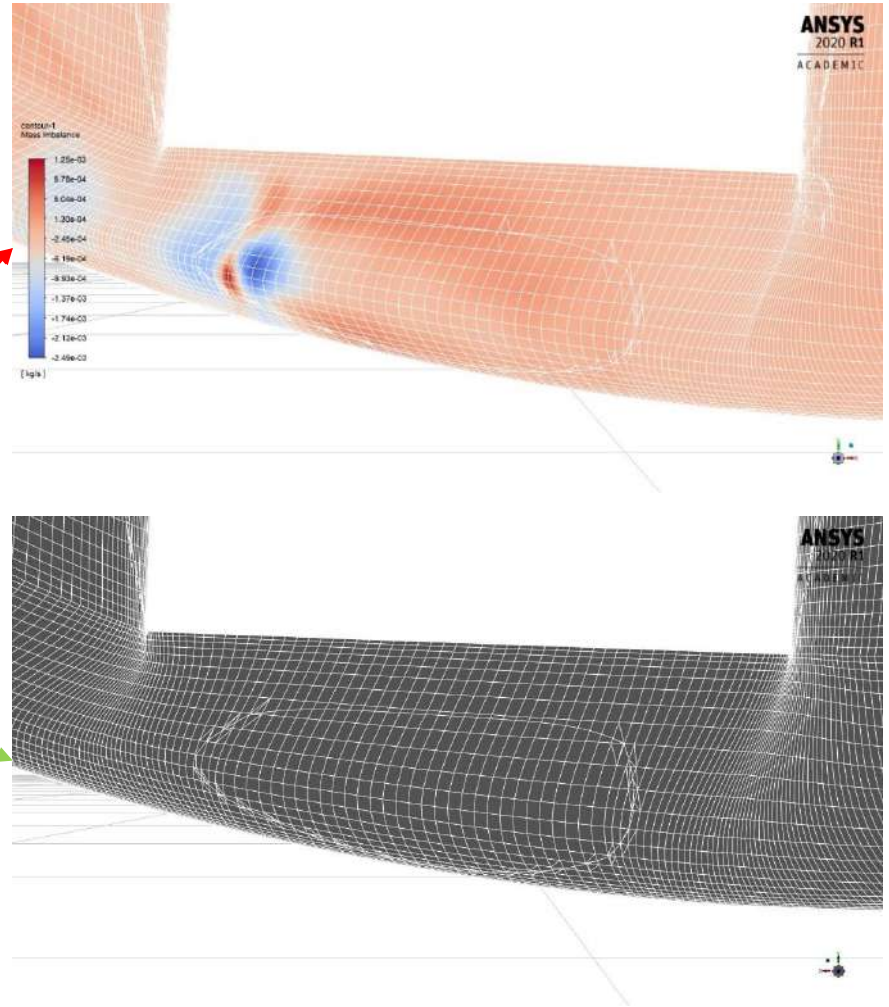

FSI analysis results:

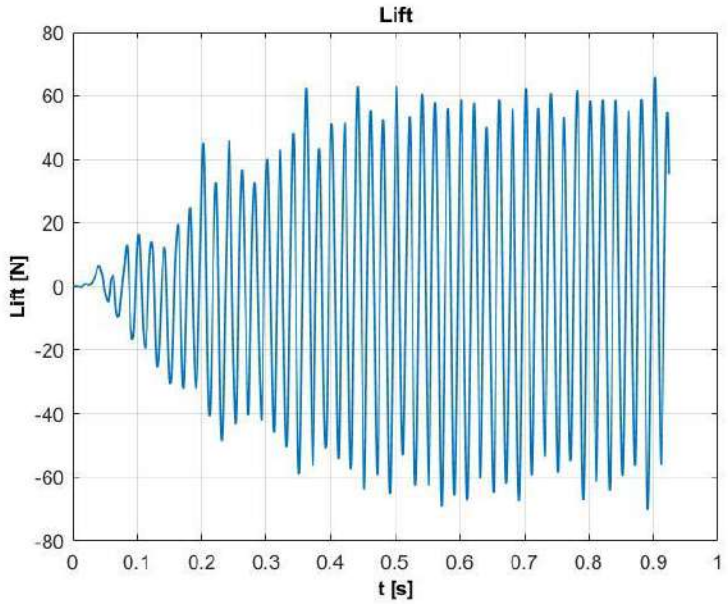

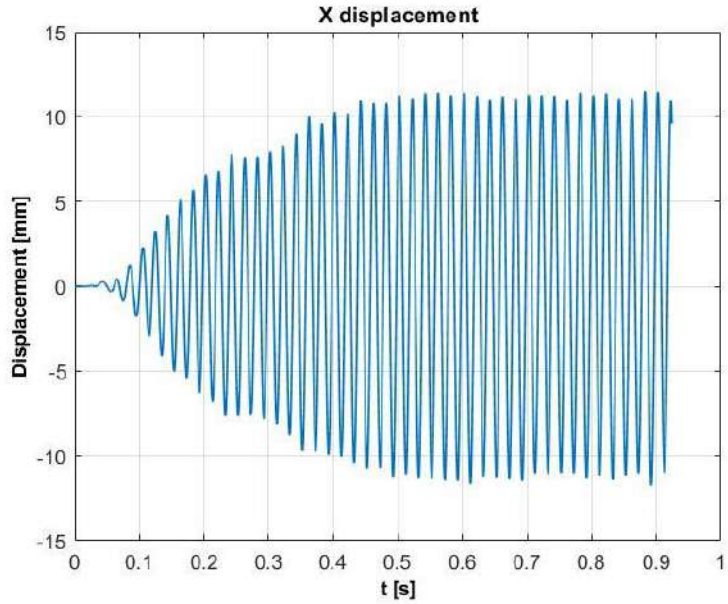

Synchronization between the vortex shedding and the thermowell oscillation ⇒ lock-in ⇒ vortex induced vibration.

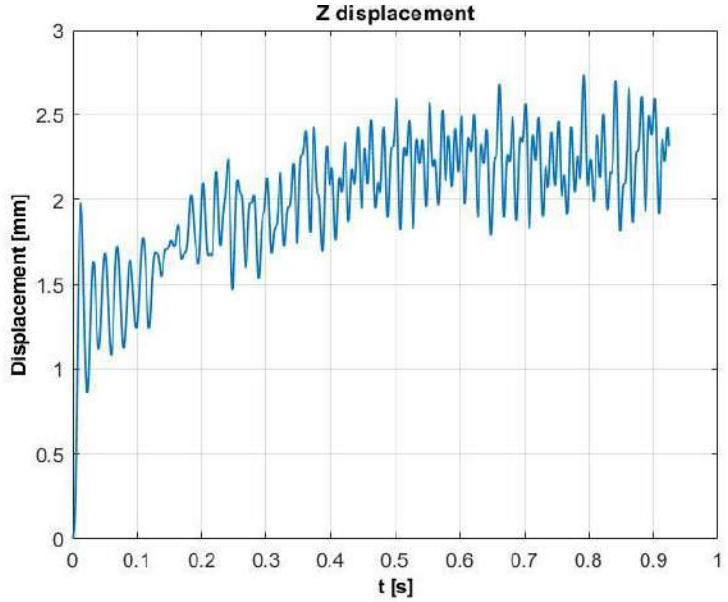

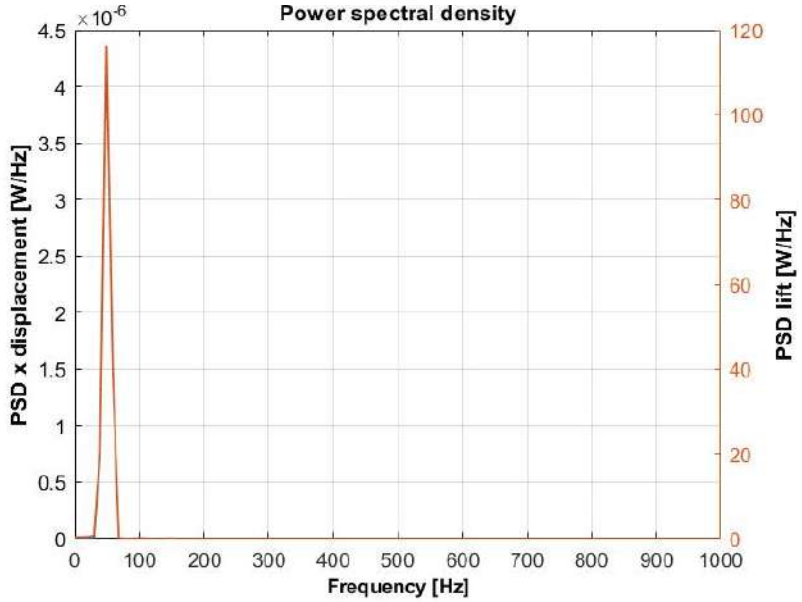

Both signals are characterized by a dominant frequency of 48.8 Hz, close to the first natural frequency of the thermowell as expected from the obtained resonance but with some deviation caused by the structural and the water damping.

In an unsteady FSI analysis using the modal superposition approach the modes truncation is performed retaining only the excited modes ⇒ the excitation on the thermowell is the lift generated by the vortex shedding, characterized by a frequency close to the one associated with the first bending mode of the structure ⇒ the retention of the first two computed natural modes would be sufficient, but the first six modes were retained for the sake of safety.

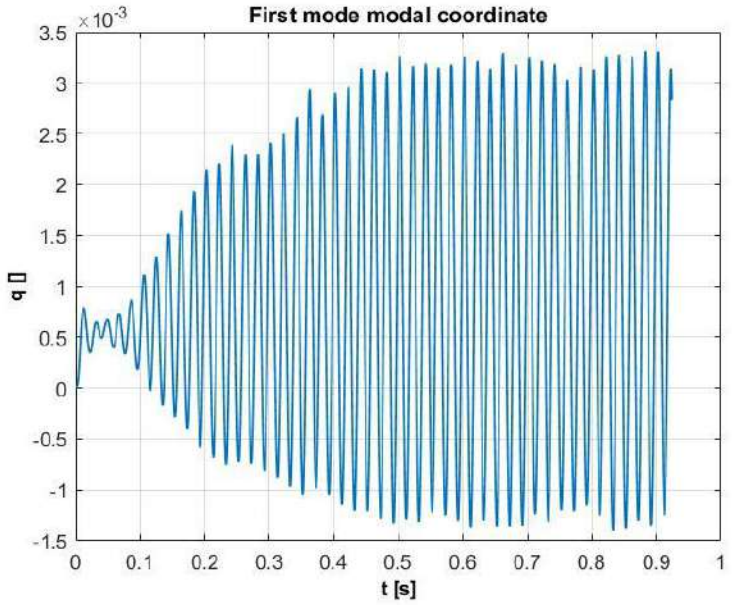

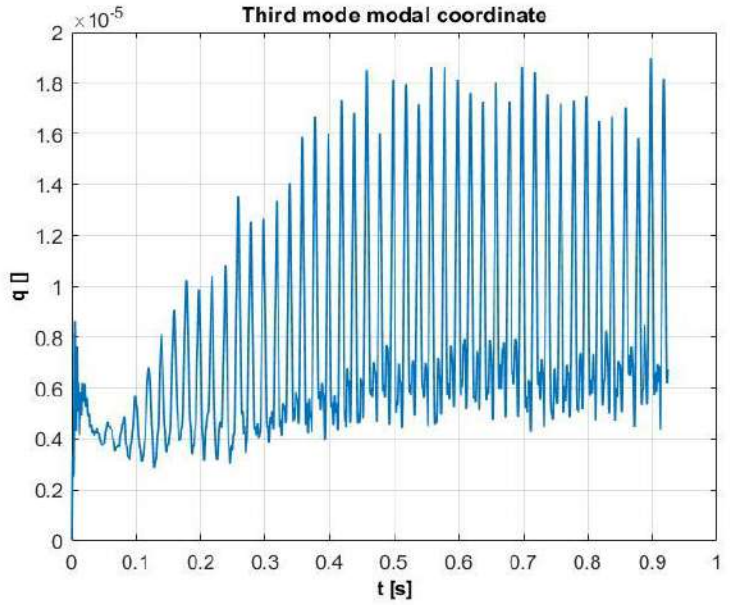

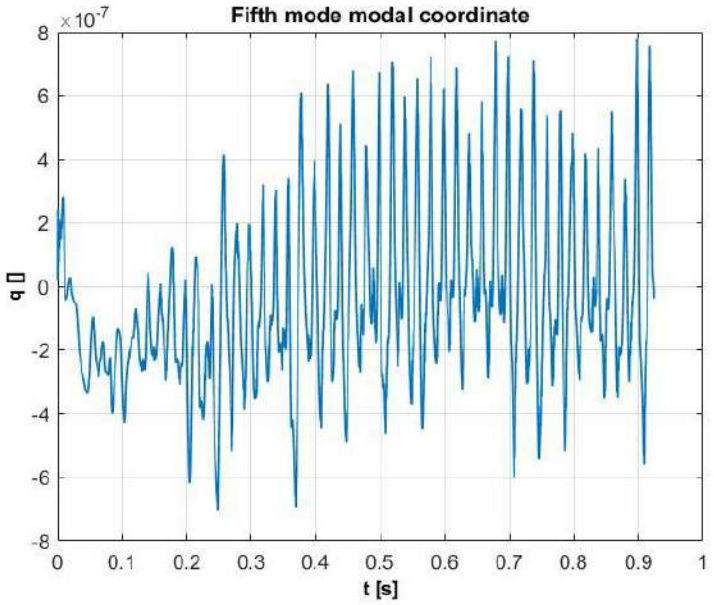

The difference in the order of magnitude between the modal coordinates associated with the different modes is clearly visible, confirming the negligible influence of the higher-frequency modes.

Vortex induced vibration animation:

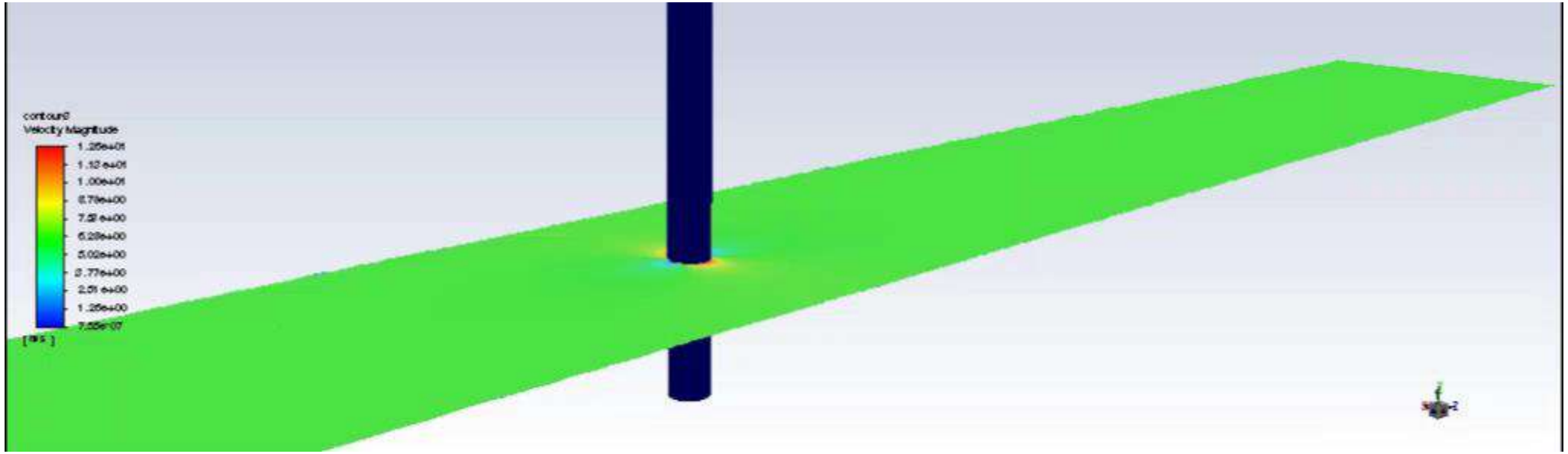

Conclusions

- From the exposed results it appears clear that the objective of the presented work was successfully achieved: by properly setting up the modal superposition method for the FSI analysis, it was possible to accurately simulate the vortex induced vibration of the thermowell, obtaining results in good agreement with the experimental data;
- The presented work demonstrated the reliability, the accuracy and the robustness of the proposed FSI transient solver, other than its speed and potential to be applied to complex industrial problems;
- Further developments:
  - Gathering more comprehensive experimental data;
  - Analysis of other fluid velocity to capture the lock-in region of the in-line vibration and the lock-off regions;
  - Analysis with different mesh setups and turbulence models (sensitivity study);
  - Submerged natural modes calculation;
  - Assessment of the non-linearities influence on the system dynamics.

Università di Roma Tor Vergata

Grazie per l'attenzione!